Charge transfer leading to multiple ionization of neon, sodium, and magnesium

R. D. DuBois
Pacific Northwest Laboratory, Richland, Washington 99352
(Received 2 May 1986)

Absolute cross sections for proton and helium-ion impact on neon, sodium, and magnesium are presented. By using coincidence techniques cross sections for pure single- or double-electron capture are separated from those events where one or more ionizations accompany the capture process. In addition, information about the direct-ionization channel is presented. The present data are combined with previous experimental information to identify specific channels which contribute to the cross sections presented here.

I. INTRODUCTION

Ion-atom collisions produce target ions as a result of either electron capture or direct Coulomb ionization. When the projectile velocity is comparable to, or smaller than, the bound target-electron velocity, capture of that electron by the projectile is the most probable process. Quite often, additional target ionization accompanies the electron-capture process, leaving the target multiply ionized.

There are several different methods by which electron capture can lead to multiple ionization of an atom. For large impact energies where the projectile velocity is comparable to, or larger than, that of an inner-shell electron, that electron may be captured, and the subsequent Auger cascades can produce relatively high degrees of ionization. In this case, it has been shown that multiple target ionization is more probable than single target ionization.[1] For very low impact energies, inner-shell electron capture is negligibly small with respect to outer-shell capture. In this case, multiple ionization occurs predominantly via the "transfer ionization" process. Here, in some cases, the charge-transfer process is exoergic. This excess energy, which can be calculated by the difference of the ionization potentials before and after the collision, is available to ionize additional target electrons. In the case of slow highly-charged ion impact, large ionization potentials are involved, and the transfer ionization process is an effective method for producing high degrees of target ionization. However, even for He^{2+} impact, it has been shown[2] that the transfer ionization channel (single-electron capture plus ionization channel) can exceed the pure single-electron-capture channel.

For intermediate energies, inner-shell electron capture is still relatively unimportant with respect to outer-shell capture, but now the projectile has sufficient kinetic energy to produce additional outer-shell ionization through direct Coulomb excitation. This "capture-plus-ionization" (C + I) process has been experimentally investigated for single-electron capture in H^+ and He^+ collisions with rare-gas atoms.[1,3–7] For these collision systems C + I can be quite important, but pure electron capture still dominates. However, for He^{2+} impact it was recently shown[8] that C + I can exceed pure electron capture in both the single and double capture channels.

It is the purpose of the present paper to investigate charge-transfer interactions for H^+, He^+, and He^{2+} impact on neon, sodium, and magnesium. The total charge-transfer cross sections are broken into their constituents, namely, pure charge transfer and charge transfer plus one or more additional ionizations. The targets presented here have outer-shell electronic configurations consisting of a filled L shell (Ne), one M shell (Na) and two M-shell electrons (Mg). Data are presented and discussed for multiple ionization of these targets associated with single-electron capture by H^+ and He^+ and for single- and double-electron capture by He^{2+} ions. In addition, since the C + I channels liberate electrons to the continuum, total electron-production cross sections are included to provide an indication of the contribution of the C + I channels to the total electron production.

A specific goal of this paper is to identify, whenever possible, and present absolute cross sections for channels leading to pure single and double capture channels, to single capture-plus-ionization channels, and to double capture-plus-ionization channels. This will be done by using new data as well as previously published cross sections to determine the relative importance of various possible channels. In cases where cross sections are not available for some of the possible channels being considered, data for other projectiles and/or targets will be used to provide indications as to which channels may be the most important.

II. EXPERIMENTAL PROCEDURE

The apparatus and procedures used in this work have been described previously[3,8,9] and will be discussed only briefly here. A collimated, momentum-analyzed ion beam was passed through a diffuse atomic beam and was then electrostatically charge-state analyzed and detected by channel electron multipliers. Slow target ions were extracted perpendicular to the projectile and target beams. The target-ion charge states were identified by their flight times between the interaction region and the target-ion detector. Coincidences between these slow ions and the postcollision projectile beams provided identification and separation of the pure electron-capture channels from the

capture-plus-ionization channels.

The following capture, capture-plus-ionization *and* ionization reactions were studied: for single capture

$$\begin{bmatrix} H^+ \\ He^+ \\ He^{2+} \end{bmatrix} + T \rightarrow \begin{bmatrix} H^0 \\ He^0 \\ He^+ \end{bmatrix} + T^+ ,$$

double capture

$$He^{2+} + T \rightarrow He^0 + T^{2+} ,$$

single capture plus ionization

$$\begin{bmatrix} H^+ \\ He^+ \\ He^{2+} \end{bmatrix} + T \rightarrow \begin{bmatrix} H^0 \\ He^0 \\ He^+ \end{bmatrix} + T^{q+} + (q-1)e , \quad q > 1 ,$$

double capture plus ionization

$$He^{2+} + T \rightarrow He^0 + T^{q+} + (q-2)e , \quad q > 2 ,$$

and ionization

$$\begin{bmatrix} H^+ \\ He^+ \\ He^{2+} \end{bmatrix} + T \rightarrow \begin{bmatrix} H^+ \\ He^+ \\ He^{2+} \end{bmatrix} + T^{q+} + qe ,$$

where T represents the targets Ne, Na, or Mg.

The coincidence signal S_q^{if} (where q is the final charge state of the target; i and f are the initial and final charge states of the ion beam) was measured for each of the reactions indicated above. The measured coincidence signal S_q^{if} is proportional to the cross section, σ_q^{if}, the beam intensity, I; the target density, N; the slow-ion-detection solid angle, $\Delta\Omega(q)$; and the detection efficiency for both slow, $\eta_s(q)$, and fast, $\eta_f(f)$, ions. Note that both the detection solid angle and detection efficiency may depend on the slow ion charge state. Thus we have

$$S_q^{if} = K\sigma_q^{if} NI\Delta\Omega(q)\eta_s(q)\eta_f(f) , \tag{1}$$

where K is a proportionality constant. In this notation, $f = i$, $i-1$, and $i-2$ for pure ionization, single, and double capture, respectively. Tests were run to demonstrate that for the experimental parameters used, the slow ion detection was independent of the slow ion charge state. In addition, the beam detection efficiency was measured as unity for 100–200-keV neutral, singly, and doubly charged ions (see Ref. 10 for details). Thus,

$$S_q^{if} = K\sigma_q^{if} NI\Delta\Omega\eta_s . \tag{2}$$

By simultaneously recording the coincidence signals for single and double charge transfer we note that the total single-charge-transfer cross section is given by

$$\sigma^{i,i-1} = \sum_q \sigma_q^{i,i-1} , \tag{3}$$

or, from Eq. (2),

$$\sigma^{i,i-1} = \sum_q S_q^{i,i-1}/(KNI\Delta\Omega\eta_s) . \tag{4}$$

Equations (2) and (4) combine to give

$$\sigma_q^{10} = \frac{\sigma^{10}}{\sum_q S_q^{10}} S_q^{10} , \tag{5}$$

$$\sigma_q^{2l} = \frac{\sigma^{2l}}{\sum_q S_q^{2l}} S_q^{2l} . \tag{6}$$

This places the single-electron-capture yields on an absolute scale, by using known single-electron-capture cross sections. The same normalization can be applied to the double capture yields since they were recorded simultaneously. Thus, double-electron-capture cross sections are given by

$$\sigma_{q'}^{20} = \frac{\sigma^{2l}}{\sum_q S_q^{2l}} S_{q'}^{20} . \tag{7}$$

Note that in the case of double capture, $q' \geq 2$ unless multiple collisions occur, in which case the ion may be neutralized in a two-step process:

$$He^{2+} + T \rightarrow He^+ + T^+ \searrow + T \rightarrow He^0 + T^+ .$$

Thus double-collision processes are distinguishable, since a singly charged target ion will then be measured in coincidence with a projectile that has captured two electrons. This can be an important feature of the coincidence technique for low-energy collisions where multiple collisions may make interpretation of charge-transfer measurements extremely difficult or unfeasible.

For the present work, absolute cross sections σ^{10} and σ^{21} were taken from Refs. 10 and 11. Using these cross sections and the procedure outlined, the coincidence cross sections σ_q^{if} are believed to be accurate to approximately 20% for the pure single capture channel, with larger uncertainties ($\sim 50\%$ or larger) for the highest charge states and smallest cross sections measured. These values include statistical as well as normalization uncertainties. Previous work[8,9] has indicated that this method of normalization may tend to overestimate the double capture cross sections for some unexplainable reason (see Ref. 8 for details). However, since no experimental uncertainties could be identified that would affect only the double capture cross sections, and since the total double capture cross sections have inherently larger uncertainties than do the total single capture cross sections, it was decided to use the normalization procedure as a best estimate of their absolute values.

Total electron-production cross sections σ_- can be derived from these data by

$$\sigma_- = \sum_q q\sigma_q^{ii} + \sum_{q>1} (q-1)\sigma_q^{i,i-1} + \sum_{q>2} (q-2)\sigma_q^{i,i-2} . \tag{8}$$

In the case of neon, the individual cross sections σ_-, σ_q^{ii}, $\sigma_q^{i,i-1}$, $\sigma_q^{i,i-2}$ have all been measured.[3,9] However, for sodium and magnesium, the target densities were too small to measure the direct ionization cross sections σ_q^{ii}, therefore the following procedure was used to obtain ionization information. The total number of slow target ions

(n) (noncoincidence) was measured simultaneously with the coincidence signals ($S_q^{i,i-1}$,$S_q^{i,i-2}$) which are the number of target ions created by electron transfer to the projectile. Since the beam-particle-detection efficiencies were measured to be unity, and the slow-ion-detection efficiency was assumed to be independent of the interaction process, e.g., direct ionization, single or double charge transfer, the following equation applies:

$$n = k \sum_q (S_q^{ii} + S_q^{i,i-1} + S_q^{i,i-2}) . \quad (9)$$

This can be used to determine the *number* of ions due to direct target ionization ($\sum_q S_q^{ii}$) from the measured total slow-ion signal (n) and the coincidence S_q^{ii} cross sections.

These relative numbers were then converted to absolute cross sections by again normalizing to the total single-charge-transfer cross sections:

$$\sum_q \sigma_q^{ii} = \frac{\sigma^{i,i-1}}{\sum S_q^{i,i-1}} \sum_q S_q^{ii} . \quad (10)$$

These ionization cross sections represent the sum of the cross sections for direct ionization to all target charge states which differ from the total electron production cross section σ_- by the contributions from direct multiple ionization and charge transfer-plus-ionization channels. In cases where direct multiple ionization can be neglected, in particular for very-low-Z target atoms $\sum_q \sigma_q^{ii} \approx \sigma_1^{ii}$, and can therefore be compared with theoretical calculations that do not include multiple ionization events. The method described above was used previously to obtain ionization cross sections for lithium[9] where good agreement was obtained with ionization cross sections measured by Shah *et al.*[12] However, because of the indirect procedure used to obtain the ionization cross sections presented here, uncertainties as large as 50% may exist. Also, the dominance of the charge transfer channels did not allow accurate ionization measurements to be performed for low impact energies.

III. RESULTS

Figures 1–3 present charge transfer and ionization cross sections for H^+, He^+, and He^{2+} impact on Ne, Na, and Mg. The total single- and double-charge-transfer cross sections (σ^{10},σ^{21}, σ^{20}), are broken down into their pure single- and double-charge-transfer cross sections (σ_1^{10},σ_1^{21},σ_2^{20}) and their charge-transfer-plus-ionization cross sections ($\sigma_{q>1}^{10}$, $\sigma_{q>1}^{21}$, $\sigma_{q>2}^{20}$) that comprise them. Also included are cross sections for total electron production, σ_-, for direct single target ionization, σ_1^{11}, and σ_1^{22}, as well as cross sections for the sum of the direct target ionization channels, $\sum_q \sigma_q^{11}$ and $\sum_q \sigma_q^{22}$, for Na and Mg targets. The cross sections are shown graphically versus the impact energy divided by projectile mass in order to more easily make comparisons of different projectiles. Where the projectile velocity matches that of the various bound target electrons are indicated by arrows at the abscissa, since this is energy in which capture of those particular electrons is expected to maximize.

Before discussing the various systems in detail, some general features of the cross sections are worth mentioning. For impact velocities less than the velocity of the

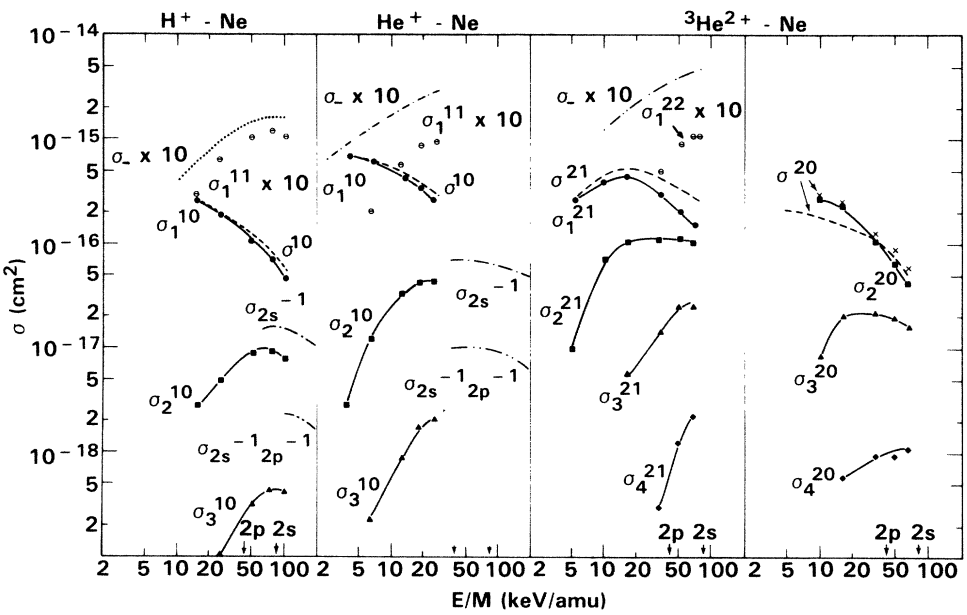

FIG. 1. Ionization and charge transfer cross sections for H^+, He^+, and He^{2+} impact on neon. Ionization: total electron production, σ_-; H^+, . . . , Ref. 13; He^+, —·—·—·, Ref. 14; He^{2+}, —··—, Ref. 11. Single direct ionization Θ ; σ_1^{11}, H^+, He^+, Ref. 3; σ_1^{22}, He^{2+}, Ref. 8. Charge transfer: total — — —; σ^{10}, H^+, He^+, Ref. 3; σ^{21}, σ^{20}, Ref. 11; σ^{20}, ×, Ref. 8. Pure charge transfer σ_1^{10} and σ_1^{21}, ●; σ_2^{20}, ■; H^+; He^{2+}, Ref. 8. Charge transfer-plus-ionization: σ_q^{10} and σ_q^{21}, $q>1$ and σ_q^{20}, $q>2$; H^+, He^+, Ref. 3; He^+, Ref. 3; He^{2+}, Ref. 8. Total $2s$ and $2s2p$ vacancy production $\sigma(2s^{-1})$ and $\sigma(2s^{-1}2p^{-1})$; Refs. 15, 16, and 18. Equivalent velocities of bound $2s$ and $2p$ target electrons indicated by arrows.

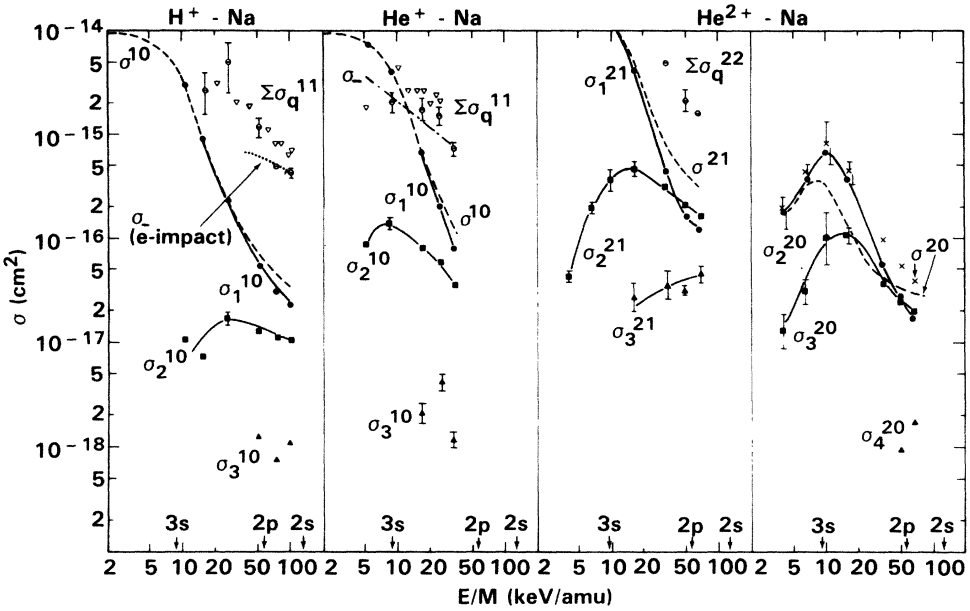

FIG. 2. Ionization and charge transfer cross sections for H^+, He^+, and He^{2+} impact on atomic sodium. Ionization: $\sum_q \sigma_q^{ii}$ (see text for explanation); Θ, present results; ▽, Ref. 22; σ_- electron impact, . . . , Refs. 19 and 20; He^+ —·—·—·, Ref. 21. Charge transfer: total — — —; σ^{10},σ^{21},σ^{20}, Ref. 10; σ^{20}, ×, present results; pure charge transfer ●, and charge transfer plus ionization ■; ▲, present results. Equivalent velocities of bound $3s$, $2p$, and $2s$ electrons are indicated by arrows.

outermost bound electron, charge transfer is more probable than is direct ionization. (See Fig. 1; note that the ionization cross sections have been multiplied by 10.) For impact velocities larger than the outermost electron velocity, the opposite is true. A change in slope occurs in the cross section curves for pure single capture (σ_1^{10} and σ_1^{21}) and to some extent in pure double capture σ_2^{20} in sodium, but not in magnesium, targets. However, it is observable in the capture-plus-ionization channels (σ_2^{10}, σ_2^{21}, and σ_3^{20}) for both Na and Mg targets. Since this change in slope occurs for projectile velocity nearly matching the L-shell bound-electron velocities it is an indication than an inner-

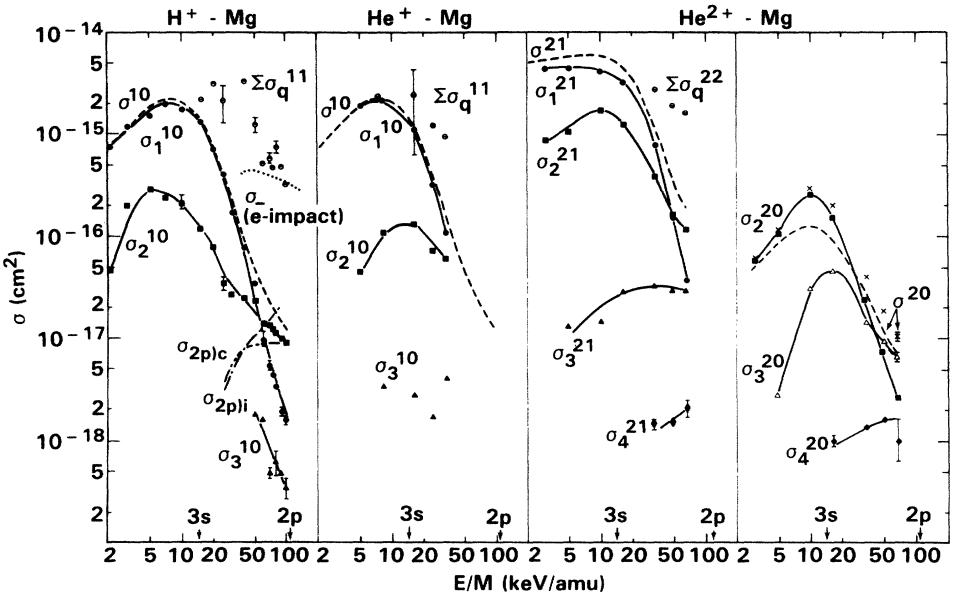

FIG. 3. Ionization and charge transfer cross sections for H^+, He^+, and He^{2+} impact on atomic magnesium. Ionization: $\sum_q \sigma_q^{ii}$ (see text for explanation); Θ, present results; σ_-, for electron impact, . . . , Ref. 20; $2p$ ionization, $\sigma(2p)_i$, —·—·—·, from Ref. 28 divided by 3.5 as explained in text. Charge transfer: total — — —; $\sigma^{10}\sigma^{21}$,σ^{20}, Ref. 10; σ^{20}, ×, present results; $2p$ capture, —··—, Ref. 28 divided by ~3.5 as explained in text. Pure charge transfer σ^{10},σ^{21}, ●, and σ^{20}, ■, Ref. 10; σ^{20}, ×, present results. Charge transfer plus ionization σ_2^{10}, σ_3^{10}, $\sigma_{q>1}^{21}$, $\sigma_{q>2}^{20}$, present results. Equivalent velocities of bound $3s$ and $2p$ electrons are indicated by arrows.

shell contribution to the capture cross section is becoming important. The reason that it is not seen for the Mg σ_1^{10}, σ_1^{21}, and σ_2^{20} cross sections will be explained in detail later.

At the higher energies, comparison of pure single-charge-transfer cross sections for the individual targets shows that equivalent velocity H^+ and He^+ impact cross sections are approximately identical and are a factor of 2—4 times smaller than for He^{2+} impact. Comparing data for different targets shows that the importance of the charge transfer-plus-ionization channels increases with respect to pure charge transfer as the target becomes heavier. In fact, for the higher energy Na and Mg data charge transfer-plus-ionization exceeds pure charge transfer.

A. Neon

The cross sections shown for neon in Fig. 1 are taken from previously published data.[3,8,11] Observe that direct single ionization σ_1^{11} and σ_1^{22} (Refs. 3 and 8) is considerably smaller than the total electron production cross sections σ_- (Refs. 11, 13, and 14) even though it has been previously shown that the direct-multiple-ionization cross sections are less than 20—30% of the direct-single-ionization cross sections.[3,8] This is because higher-order charge-transfer channels also contribute free electrons. These higher-order charge-transfer channels are considerably more important for He^{2+} impact than for H^+ or He^+ impact. The present double capture cross sections σ^{20} tend to be 30—50% larger than those measured using a growth-curve technique.[11] As was previously stated, this has been observed for other systems, and thus far, no experimental reason for this discrepancy has been identified.

It is possible to identify which target electrons and processes contribute to cross sections for direct ionization, pure charge transfer and charge transfer plus one additional ionization for neon. Neon has a $1s^2 2s^2 2p^6$ electronic configuration, but only L-shell electrons ($n=2$) can contribute to the cross sections shown in Fig. 1 since the K-shell ($n=1$) electrons are too tightly bound to be ionized by the projectile energies being considered here. Channels that may contribute to pure single and double capture, to single and double capture plus one additional ionization, and to direct ionization are as follows. The general notation used is $nl\,|_x$ where x may be either c or i for capture or ionization and l designates either s or p electrons for the targets being discussed here. Note that the values of n and l will be explicitly stated in certain cases to avoid confusion; otherwise a more general nl notation will be used.

Pure single capture	$\sigma_1^{10},\sigma_1^{21}$	$2l\,\|_c$
Single capture plus ionization	$\sigma_2^{10},\sigma_2^{21}$	$2l\,\|_c 2l\,\|_i$
Pure double capture	σ_2^{20}	$2l^2\,\|_c$
		$2p\,2s\,\|_c$
Double capture plus ionization	σ_3^{20}	$2p^2\,\|_c 2l\,\|_i$
		$2p\,2s\,\|_c 2l\,\|_i$
		$2s^2\,\|_c 2p\,\|_i$
Ionization	$\sigma_1^{11},\sigma_1^{22}$	$2l\,\|_i$

For the range of impact energies discussed here it is possible to determine which of these channels are dominant by comparing the cross sections presented here with previously published data. For example, pure single capture σ_1^{10} for H^+ and He^+ impact occurs via $2p$ capture. $2s$ capture can be neglected since the *total* $2s$ vacancy production cross sections[15,16] shown in Fig. 1 are, at most, only 25% of σ_1^{10}. It is known that direct ionization dominates the charge-transfer mechanism for Ne^+ production in this energy range;[3] thus $2s$ capture is only a small portion of this 25% and can be ignored. This conclusion is supported by theoretical calculations of $2p$ and $2s$ capture.[17] The same arguments are assumed to also hold for equivalent velocity He^{2+} impact as well.

In the case of single capture plus ionization, all channels except $2p\,|_c 2p\,|_i$ can be eliminated since the *total* $2s2p$ vacancy production cross sections[15,18] are smaller than 20% of the σ_2^{10} cross section, and the *total* $2s^2$ vacancy production is even less likely.[15,17,18] In both cases, the charge-transfer portion of these channels should represent only a portion of these total cross sections and are thus negligible with respect to σ_2^{10}. This is rigorously true only for the H^+ and He^+ impact energies shown but is assumed to be true for equivalent velocity He^{2+} impact also.

Pure double charge transfer σ_2^{20} can occur via double $2p$ capture, $2p2s$ capture, or double $2s$ capture. Although not directly verifiable with existing experimental or theoretical data, the arguments presented above imply that only the double $2p$ capture channel is important. Likewise, the most probable double capture-plus-ionization channel is the $2p^2\,|_c 2p\,|_i$.

In the case of direct ionization of neon by proton impact, the measured[3] direct-single-ionization cross sections are attributed to $2p$ ionization, since the $2s$ ionization cross sections are known to be considerably smaller.[15,17] Again, it is assumed that this also holds true for He^+ and He^{2+} impact.

B. Sodium

Cross sections for pure capture, capture plus ionization, and pure ionization or H^+-,He^+-, and He^{2+}-Na collisions are shown in Fig. 2. The influence of inner-shell contribution to the capture cross sections is indicated by a change in slope of the cross sections for impact velocities near the velocity of the sodium L-shell electrons. This is most evident for pure single capture σ_1^{10} and σ_1^{21} by H^+ and He^{2+} and, to a lesser extent, in the pure double capture σ_2^{20} and the capture-plus-ionization cross sections σ_2^{10}, σ_2^{21} and σ_3^{20}. In the case of high-energy He^{2+} impact, the charge transfer-plus-ionization cross section exceeds the pure charge-transfer cross section, both in the single and double capture channels. This has been previously observed for He^{2+}-Ar, -Kr collisions.[8] Again we note that the present total double capture cross sections (x) are 30—100% larger than those measured using the growth-curve method (dashed line[10]).

The proton-impact ionization cross sections shown in Fig. 2 agree reasonably well with electron-impact data[19,20] at higher energies and with the He^+ impact ionization

calculations of Tiwary and Rai.[21] However, comparison of these data for H^+ and He^+ ionization of sodium with cross sections deduced from the data of O'Hare *et al.*[22] shows that these data are smaller by approximately a factor of 2. This is similar to results we previously reported[10] for total single-charge-transfer cross sections where the data of O'Hare *et al.* were approximately two times larger than our measurements as well as those of others. This could indicate that their target density measurements were inaccurate.

In order to interpret the cross sections presented in Fig. 2 we note that sodium has an electronic configuration of a neonlike core plus an additional outer-shell electron, i.e., a $1s^2 2s^2 2p^6 3s$ configuration. Since the K-shell electrons are so tightly bound that they can be ignored in the interactions reported here, and since the neon data showed that it is probably safe to also ignore the $2s$ contributions with respect to the $2p$ influence, the channels that might contribute to the cross sections shown in Fig. 2 are

Pure single capture	$\sigma_1^{10}, \sigma_1^{21}$	$3s \mid_c$
		$2p \mid_c$ leading to $3s \rightarrow 2p$ photon deexcitation
Single capture plus ionization	$\sigma_2^{10}, \sigma_2^{21}$	$3s \mid_c 2p \mid_i$
		$2p \mid_c 3s \mid_i$
		$2p \mid_c 2p \mid_i$ with $3s \rightarrow 2p$ photon deexcitation. autoionization channels
		$2p \mid_c 2p$ excitation
		$2s \mid_c$
		$2s \mid_c 3s$ excitation
Pure double capture	σ_2^{20}	$2p\,3s \mid_c$
		$2p^2 \mid_c$
Double capture plus ionization	σ_3^{20}	$2p\,3s \mid_c 2p \mid_i$
		$2p^2 \mid_c 3s \mid_i$
Ionization	$\sigma_1^{11}, \sigma_1^{22}$	$3s \mid_i$
		$2p \mid_i$

As pointed out earlier, both the $3s$ and the $2p$ capture channels contribute to the pure single-electron-capture cross section. The contribution from $2p$ capture is observed as a change in slope in the projectile velocity dependence for projectile velocities that nearly match the bound L-shell electron velocities. At lower energies, $3s$ capture should dominate, with $2p$ capture becoming important above approximately 30 keV/amu. Note that following $2p$ capture, a $3s \rightarrow 2p$ photon transition will occur.

In the case of ionization, previous data[22] have shown that direct double ionization is small with respect to single ionization. However, insufficient information is available to determine the relative importance of $3s$ and $2p$ ionization—both of which probably contribute, as in the pure single capture case.

For single capture plus ionization several channels could contribute to the measured cross sections. Of the channels listed, some information about those leading to autoionization is known. For example, many autoionizing transitions have been identified,[23–25] and relative autoionization intensities have been measured for H^+ and He^+ (Ref. 26) impact. In the case of H^+ impact, it is possible to place the relative intensities for transitions leading to double ionization of sodium on an absolute scale (subject to uncertainties of a factor of 2 or 3) by normalizing to the total absolute $2p^5 3s^2(^2P) \rightarrow 2p^6(^1S_0)$ intensity, which has recently been measured.[27] Doing so yields a total autoionization contribution to double ionization of sodium of approximately 5×10^{-18} cm^2 for proton energies between 50 and 300 keV.

This value is not totally inconsistent with the measured σ_2^{10} value of approximately 1×10^{-17} cm^2. However, the autoionization intensity of approximately 5×10^{-18} cm^2 results from both capture *and* ionization processes, whereas the present σ_2^{10} value of 1×10^{-17} cm^2 is due only to capture events. It will be shown in the next section, for H^+-Mg collisions, that the $2p$ ionization cross section is approximately twice the $2p$ capture cross section for velocities equal to the bound $2p$ electron velocity. Assuming this to be approximately the same for H^+-Na collisions, the autoionization channels probably account for less than 25% of the measured σ_2^{10} cross section for H^+ impact on sodium.

This would leave the $3s \mid_c 2p \mid_i$, $2p \mid_c 3s \mid_i$, and $2p \mid_c 2p \mid_i$ channels to be primarily responsible for the observed σ_2^{10} and σ_2^{21} cross sections. However, one would expect that the removal of two electrons is much less probable than the removal of either electron alone, e.g., $3s \mid_c 2p \mid_i \ll 3s \mid_c$, $2p \mid_c 3s \mid_i$, and $2p \mid_c 2p \mid_i \ll 2p \mid_c$. Thus, we would expect that $\sigma_2^{10} < \sigma_1^{10}$ and $\sigma_2^{21} < \sigma_1^{21}$. Since the higher-energy He^{2+} results show that $\sigma_2^{21} > \sigma_1^{21}$, either autoionization plays a larger role than estimated, or some of our assumptions are invalid, or the combined effect of the capture-plus-ionization channels for He^{2+} impact is larger than that of the pure capture channels. Additional experimental or theoretical analysis is required to resolve this question.

In the case of double capture, $\sigma_3^{20} > \sigma_2^{20}$ at higher energies. The pure double capture channels are $3s\,2p$ capture and double $2p$ capture, both of which will be associated with a $3s \rightarrow 2p$ photon relaxation. As was the case for proton impact, both channels are probably important, since the cross section changes slope at higher energies. For double capture-plus-ionization, both the $2p\,3s \mid_c 2p \mid_i$ and $2p^2 \mid_c 3s \mid_i$ are expected to be smaller than the pure double capture channels, $2p\,3s \mid_c$ and $2p^2 \mid_c$. Thus, in order that $\sigma_3^{20} > \sigma_2^{20}$ at higher impact energies, there may be important unidentified autoionization transitions contributing to σ_3^{20} or, possibly, channels such as $2s$ capture that need to be considered.

C. Magnesium

Cross sections for magnesium are shown in Fig. 3. For the case of ionization, the data for electron impact[28] appear to merge smoothly with the H^+ results at higher en-

ergies. Note that the $2p\,|_i$ and $2p\,|_c$ cross sections shown in Fig. 3. have been reduced by a factor of approximately 3.5 from those presented in Ref. 29 in order to make the $2p$ capture cross sections consistent with the σ_2^{10} cross sections presented here and because $2p$ capture cannot exceed the total single-electron-capture cross section σ^{10}, taken from Ref. 10. It is assumed that the $2p$ cross sections presented in Ref. 29 are overestimated in absolute value because of the normalization process that was used.

As was observed for sodium, the ionization cross sections are considerably larger than the charge-transfer cross sections. Also, the dominance of capture-plus-ionization over pure capture at higher energies is quite obvious.

In order to identify the specific channels leading to ionization, capture, and capture-plus-ionization, we note that magnesium has a $1s^2 2s^2 p^6 3s^2$ electronic configuration. For the energy range presented here, only the $2p$ and $3s$ electrons are expected to contribute to the cross sections. Thus, the various available channels ionization are

Pure single capture	$3s\,\|_c$
Single capture plus ionization	$3s\,\|_c 3s\,\|_i$ $3s\,\|_c 2p\,\|_i$ $2p\,\|_c 3s\,\|_i$ $2p\,\|_c +$ Auger relaxation
Pure double capture	$3s^2\,\|_c$ $2p\,3s\,\|_c$ with $3s$-$2p$ photon
Double capture plus ionization	$3s^2\,\|_c 2p\,\|_i$ $2p\,3s\,\|_c 3s\,\|_i$ $2p\,3s\,\|_c 2p\,\|_i$ $2p^2\,\|_c 3s\,\|_i$ $2p^2\,\|_c +$ Auger relaxation
Ionization, single double	$3s\,\|_i$ $3s^2\,\|_i$ $2p\,\|_i +$ Auger relaxation

Note that pure single electron capture from magnesium can occur *only* via the $3s\,|_c$ channel, since $2p$ capture would lead to double target ionization via Auger relaxation. Hence, the σ_1^{10},σ_1^{21} cross sections show a rapid decrease for impact velocities considerably larger than the $3s$ binding energy.

The ionization cross sections shown for magnesium most likely result from single $3s$ ionization, since double $3s$ ionization is considered to be much less likely, and $2p$ ionization is shown to be small with respect to the measured ionization cross sections. As noted previously in this paper, this is rigorously true only for H^+ impact but is assumed to be valid for the He^+ and He^{2+} collision systems also.

Single capture-plus-ionization can occur via several different channels. At lower impact energies only the $3s\,|_c 3s\,|_i$ channel contributes, since all other channels have contributions from $2p$ electrons, and the $2p$ cross sections are shown to be relatively small for lower impact energies. At higher energies, it is shown that $3s\,|_i$, i.e., $\sum_q \sigma_q^{11}$, is much larger than $2p\,|_i$. Thus $3s\,|_c 3s\,|_i \gg 3s\,|_c 2p\,|_i$. Also at higher energies, since it is also assumed that $2p\,|_c 3s\,|_i$ is less probable than $2p\,|_c$ alone, and since $3s\,|_c$ (i.e., σ_1^{10}) is small with respect to $2p\,|_c$ (see Fig. 3), this leaves only the $2p\,|_c$ channel to account for the higher energy σ_2^{10} cross section. It is the inclusion of this inner-shell capture channel that causes σ_2^{10} to exceed σ_1^{10}, as seen in Fig. 3. Again, these arguments and conclusions are for H^+-Mg collisions but it is expected that cross sections for equal velocity He^+ and He^{2+} impact will behave in the same manner.

In the double capture channels we again have the situation, as was seen for the sodium target, that the capture-plus-ionization cross section is larger than the pure double capture cross section at higher energies. The only pure double capture channels are $3s^2\,|_c$ and $2p\,3s\,|_c$, both of which may contribute. However, $3s^2\,|_c 2p\,|_i$, $2p\,3s\,|_c 3s\,|_i$, $2p\,3s\,|_c 2p\,|_i$, $2p^2\,|_c 3s\,|_i$, $2p^2\,|_c$ followed by Auger relaxation are possible double capture-plus-ionization channels. Of these, $2p\,3s\,|_c 2p\,|_i \ll 2p\,3s\,|_c 3s\,|_i$ since $2p\,|_i \ll 3s\,|_i$. Also, it is expected that $2p^2\,|_c 3s\,|_i \ll 2p^2\,|_c$. At lower impact energies, $2p^2\,|_c$ is expected to be negligible with respect to $3s^2\,|_c 2p\,|_i$ and $2p\,3s\,|_c 3s\,|_i$, but it is not possible to determine the relative importance of these latter two terms. At higher energies it has been shown that $3s\,|_c \ll 2p\,|_c$; this means that $2p\,3s\,|_c 3s\,|_i \ll 2p^2\,|_c 3s\,|_i$, which is small with respect to $2p^2\,|_c$. Also, it is expected that $3s^2\,|_c 2p\,|_i \ll 2p^2\,|_c$ since $3s\,|_c \ll 2p\,|_c$. Hence, the most likely channels leading to double capture-plus-ionization are $3s^2\,|_c 2p\,|_i$ and $2p\,3s\,|_c 3s\,|_i$ at lower energies and, at higher energies, double $2p$ capture followed by Auger relaxation. Again, it is likely that the inclusion of inner-shell capture followed by Auger relaxation causes σ_3^{20} to be larger than σ_2^{20} at higher energies. However, such transitions have not been identified thus far.

IV. CONCLUSIONS

Cross sections for pure single and double capture, single and double capture-plus-additional-ionization of one or two electrons, and information about direct ionization for H^+, He^+, and He^{2+} ions impacting on neon, sodium, and magnesium have been presented. It was observed that, for lower-energy H^+ and He^+ impact, the total single capture cross section is almost entirely due to pure single capture. But for higher impact energies, charge transfer plus ionization becomes more important and, in some cases, dominates.

In many cases it was possible to identify specific channels contributing to these cross sections. These cross sections provide the opportunity to test theoretical calculations of charge transfer in great detail.

ACKNOWLEDGMENT

The work for this paper was supported by the United States Department of Energy, Division of Magnetic Fusion Energy, under Contract No. DE-AC06-76RLO 1830.

[1]E. Horsdal-Pedersen and L. Larsen, J. Phys. B **12**, 4085 (1979).
[2]W. Groh, A. S. Schlachter, A Müller, and E. Salzborn, J. Phys. B Lett. **15**, L207 (1982).
[3]R. D. DuBois, Phys. Rev. Lett. **52**, 2348 (1984).
[4]M. B. Shah and H. B. Gilbody, J. Phys. B **18**, 899 (1985).
[5]V. V. Afrosimov, Y. A. Mamaev, M. N. Panov, and V. Uroshevich, Zh. Tekh. Fiz. **37**, 717 (1967) [Sov. Phys.—Tech. Phys. **12**, 512 (1967)].
[6]V. V. Afrosimov, Y. A. Mamaev, M. N. Panov, and N. V. Federenko, Zh. Tekh. Fiz. **39**, 159 (1969) [Sov. Phys.—Tech. Phys. **14**, 109 (1969)].
[7]B. Schuch, diplomarbeit, University of Giessen, 1984.
[8]R. D. DuBois, Phys. Rev. A **33**, 1595 (1986).
[9]R. D. DuBois, Phys. Rev. A **32**, 3319 (1985).
[10]R. D. DuBois and L. H. Toburen, Phys. Rev. A **31**, 3603 (1985).
[11]M. E. Rudd, T. V. Goffe, and A. Itoh, Phys. Rev. A **32**, 2128 (1985).
[12]M. B. Shah D. S. Elliot and H. B. Gilbody, J. Phys. B **18**, 4245 (1985).
[13]M. E. Rudd, R. D. DuBois, L. H. Toburen, C. A. Ratcliffe, and T. V. Goffe, Phys. Rev. A **28**, 3244 (1983).
[14]M. E. Rudd, T. V. Goffe, A. Itoh, and R. D. DuBois, Phys. Rev. A **32**, 829 (1985).
[15]M. Eckhardt and K-H. Schartner, Z. Phys. A **312**, 321 (1983).
[16]R. Hippler and K-H. Schartner, Z. Phys. A **273**, 123 (1975).
[17]S. T. Manson, R. D. DuBois, and L. H. Toburen, Phys. Rev. Lett. **51**, 1542 (1983).
[18]H. F. Beyer, R. Hippler, and K-H. Schartner, Z. Phys. A **292**, 353 (1979).
[19]R. H. McFarland and J. D. Kinney, Phys. Rev. A **137**, 1058 (1965).
[20]I. P. Zapesochnyi and I. S. Aleksakhin, Zh. Eksp. Teor. Fiz. **55**, 76 (1968) [Sov. Phys.—JETP **18**, 41 (1969)].
[21]S. N. Tiwary and R. K. Rai, J. Chem. Phys. **68**, 2427 (1978).
[22]B. G. O'Hare, R. W. McCullough, and H. B. Gilbody, J. Phys B **8**, 2968 (1975).
[23]D. J. Pegg, H. H. Haselton, R. S. Thoe, P. M. Griffin, M. D. Brown, and I. A. Sellin, Phys. Rev. A **12**, 1330 (1975).
[24]K. J. Ross, T. W. Ottley, V. Pejcev, and D. Rossi, J. Phys. B **9**, 3237 (1976).
[25]E. Breuckmann, B. Breuckmann, W. Mehlhorn, and W. Schmitz, J. Phys. B **10**, 3135 (1977).
[26]N. Stolterfoht, *Proceedings of the 2nd International Conference on Inner-Shell Ionization Phenomena,* edited by W. Mehlhorn and R. Brenn (Universität Freiburg, Freiburg, Germany, 1976), p. 42.
[27]G. Kessler, diplomarbeit, University of Freiburg, 1985.
[28]L. A. Vainshtein, V. I. Ochkur, V. I. Rakhovskii, and A. M. Stepanov, Zh. Eksp. Teor. Fiz. **61**, 511 (1971) [Sov. Phys.—JETP **34**, 271 (1972)].
[29]R. D. DuBois, J. P. Giese, and C. L. Cocke, Phys. Rev. A **29**, 1079 (1984).